

Case Report

Decision Support for Removing Fractured Endodontic Instruments: A Patient-Specific Approach

Raphaël Richert ^{1,2,*} , Jean-Christophe Farges ^{1,3}, Cyril Villat ^{1,4}, Sébastien Valette ^{1,5} , Philippe Boisse ² 
and Maxime Ducret ^{1,3,*}

¹ Hospices Civils de Lyon, PAM Odontologie, 69007 Lyon, France; jean-christophe.farges@chu-lyon.fr (J.-C.F.); cyril.villat@univ-lyon1.fr (C.V.); sebastien.valette@insa-lyon.fr (S.V.)

² Laboratoire de Mécanique des Contacts et Structures, UMR 5259 CNRS/INSA/Univ Lyon, 69100 Villeurbanne, France; philippe.boisse@insa-lyon.fr

³ Laboratoire de Biologie Tissulaire et Ingénierie Thérapeutique, UMR 5305 CNRS/UCBL, 69008 Lyon, France

⁴ Laboratoire des Multimatériaux et Interfaces, UMR CNRS 5615/UCBL, 69622 Villeurbanne, France

⁵ Centre de Recherche en Acquisition et Traitement de l'Image pour la Santé, UMR 5220 CNRS/INSERM U1206/INSA, 69100 Villeurbanne, France

* Correspondence: raphael.richert@insa-lyon.fr (R.R.); maxime.ducret@univ-lyon1.fr (M.D.)

Featured Application: Endodontics.

Abstract: The instrumental fracture is a common endodontic complication that is treated by surgical or non-surgical removal approaches. However, no tool exists to help the clinician to choose between available strategies, and decision-making is mostly based on clinical judgment. Digital solutions, such as Finite Element Analysis (FEA) and Virtual Treatment Planning (VTP), were recently proposed in maxillofacial surgery. The aim of the current study is to present a digital tool to help decide between non-surgical and surgical strategies in a clinical situation of a fractured instrument. Five models have been created: the initial state of the patient, two non-surgical removal strategies using a low or high root canal enlargement, and two surgical removal strategies using a 3- or 6-mm apicoectomy. Results of the VTP found a risk of perforation for the non-surgical strategies and sinus proximity for surgical ones. FEA showed the lowest mechanical risk for the apicoectomy strategy. A 3-mm apicoectomy approach was finally chosen and performed. In conclusion, this digital approach could offer a promising decision support for instrument removal by planning the treatment and predicting the mechanical impact of each strategy, but further investigations are required to confirm its relevance in endodontic practice.

Keywords: finite element analysis; virtual treatment planning; endodontics; apicoectomy; Instrument removal; decision-making



check for
updates

Citation: Richert, R.; Farges, J.-C.; Villat, C.; Valette, S.; Boisse, P.; Ducret, M. Decision Support for Removing Fractured Endodontic Instruments: A Patient-Specific Approach. *Appl. Sci.* **2021**, *11*, 2602. <https://doi.org/10.3390/app11062602>

Academic Editor: Luca Testarelli

Received: 6 February 2021

Accepted: 5 March 2021

Published: 15 March 2021

Publisher's Note: MDPI stays neutral with regard to jurisdictional claims in published maps and institutional affiliations.



Copyright: © 2021 by the authors. Licensee MDPI, Basel, Switzerland. This article is an open access article distributed under the terms and conditions of the Creative Commons Attribution (CC BY) license (<https://creativecommons.org/licenses/by/4.0/>).

1. Introduction

During cleaning and shaping of the root canal, troublesome incidents, such as the fracture of the instrument, can occur. Many factors contribute to instrument fracture, and these have been associated with torsion stress or flexural fatigue [1]. The prevention of file separation has been widely investigated and is based on inspection of the file (notably of the winding of the flutes) or curvature management, which has led to more flexible endodontic files [1]. However, the fracture of an endodontic instrument within the root canal remains a common complication of endodontic treatments (0.25 to 7.41%), with most fractures occurring in the apical third of the root [2,3]. This fracture can affect tooth prognosis, and several instrument removal strategies have been reported to complete the endodontic treatment [1,4]. A non-surgical strategy was proposed using ultrasonic tips to loosen the fractured instrument, but this procedure can lead to canal over-enlargement or root perforation [5,6]. A surgical strategy was also reported to remove the instrument after

performing an apicoectomy [7], but it induces a reduction of the crown-to-root ratio [8,9]. Both strategies thus impact mechanically the tooth and the success of the endodontic retreatment [10,11]. No tool exists, at the time of writing, to guide the clinician in choosing between these strategies, and decision-making is mostly based on clinical judgment instead of scientific evidence [3]. Furthermore, numerous different tools are available to deal with retained instruments, including mini forceps, broach and cotton, hypodermic surgical needles, wire loops, Masseran instruments, extractors, and ultrasonic tips [1,4]. In the face of the multitude of possible therapeutical choices, instrument removal is still considered highly technical and time-consuming because dental practitioners have difficulties planning the removal and its impact on tooth resistance.

Digital approaches have been used for many years; for instance, virtual treatment planning (VTP) has been used to improve the reconstruction accuracy and outcome in the maxillofacial field [12,13], and patient-specific finite element analysis (FEA) has been used to provide better predictions on bone fracture than experienced clinicians in orthopedic practice [14]. In endodontics, FEA has been used to evaluate the influence of the instrument position and the resection length on the root stress distribution [15–17]. However, these studies use standard anatomic dimensions to create finite element (FE) models, and the success rate mainly depends on patient-specific parameters such as bone loss and canal anatomy [6,9,18]. A recent study proposed combining VTP and FEA for computer-aided decision-making, with the aim to predict the mechanical behavior of different maxillofacial surgeries and choose the most adapted solution for the patient [19]. Herein, we report a case of an endodontic instrument fracture and the application of a digital approach combining VTP and FEA to help decide between surgical and non-surgical strategies for its removal.

2. Case Report

2.1. Case Presentation

A 26-year-old female patient was addressed to the department of endodontics of the Lyon University Hospital with a fractured instrument (FI) in the root canal of her right second maxillary premolar. The 8 mm-long instrument was fractured during an initial endodontic treatment of irreversible pulpitis one week previously. The patient reported no pain since the fracture occurred. Clinical examination of the premolar crown indicated the presence of four dental walls and a recent temporary restoration on the occlusal face. The tooth presented no cold response, no percussion or palpation tenderness, and physiological mobility. The intraoral periapical radiograph confirmed the transfixed position of the instrument, close to the sinus, and the absence of periapical radiolucency or local swelling of the sinus membrane (Figure 1a). The patient's tooth was scanned before any intervention to evaluate the instrument position using cone beam computed tomography (CBCT; Planmeca ProMax 3D, Helsinki, Finland) operating at 120 kV, 100 mAs, with a slice thickness of 0.75 mm. The data were recorded under the Digital Imaging and Communication in Medicine (DICOM) format and analyzed. Two non-surgical and surgical strategies emerged from the discussions of the healthcare team, but no consensus was defined on the treatment that could ensure the best outcome. A digital approach, combining VTP and FEA [19], was then implemented to visualize the planned treatment and predict the mechanical impact of the two removal strategies (Figure 1).

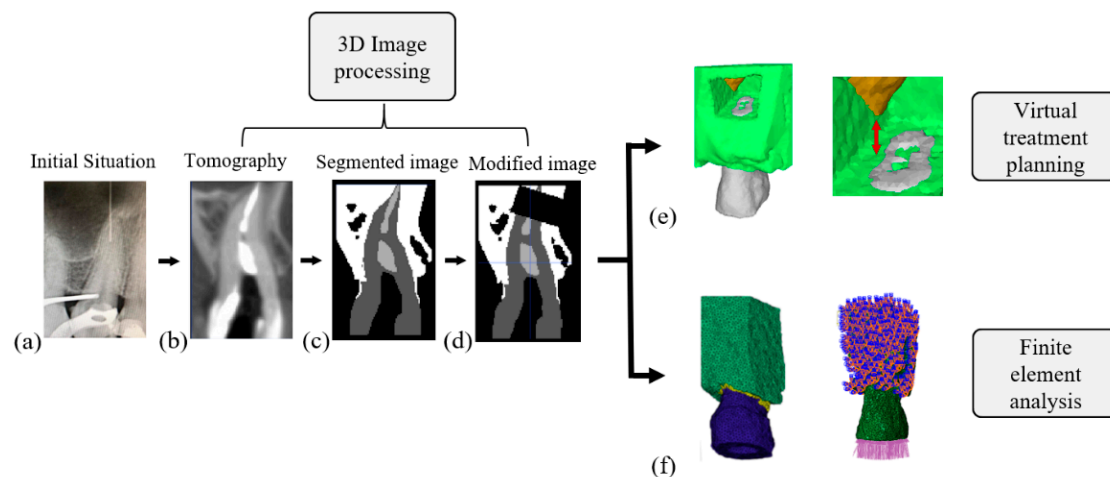


Figure 1. The process for a patient-specific biomechanical analysis and detailed steps for virtual treatment planning and finite element analysis: (a) radiograph of the initial situation presenting a fractured instrument, (b) cone beam computed tomography axial view with temporary intracanal medication, (c) segmentation based on a growing region algorithm, (d) transformation of the initial 3D image to simulate a 3 mm apicoectomy, (e) analysis of the 3D simulated treatment, and (f) meshing of the 3D transformed image to get a finite element model and application of boundary conditions.

2.2. Virtual Treatment Planning

The different anatomical structures were segmented using DESK, an application suited for medical images [20]. The semi-automatic segmentation is based on the attribution of pixel labels, “seeds”, inside each anatomical structure and a growing region algorithm. Four labels were generated according to the structures of “air”, “tooth”, “bone”, and “intra-root canal material” to produce a multi-label 3D image. This initial 3D image was then modified to simulate the procedures of the different removal strategies.

Five clinical situations were considered by the healthcare team: the initial state of the patient, two simulated non-surgical removal strategies using a low or high root canal enlargement, and two simulated surgical removal strategies using a 3 or 6 mm apicoectomy.

An ultrasonic tip (ET25; Satelec, Bordeaux, France) was modeled by a conical cylinder 0.5 mm in diameter and a 4% taper and recorded under Standard Tessellation Language (STL) format for VTP of non-surgical approaches. The surface of the tip was then superimposed along one-third of the instrument either on the distal side of the instrument to simulate a low root canal enlargement or on the distal and vestibular sides of the instrument to simulate a high root canal enlargement. VTP of surgical approaches was conducted with a 3 or 6 mm root shortening (Figure 2a).

The different virtual removal strategies were analyzed on the 3D modified image. The latter offers the operator the possibility to add or suppress masks of bone, ultrasonic tip or instrument to plan his procedure. For non-surgical strategies, the high enlargement was associated with a long perforation. VTP of surgical strategies was also informative for the reduction of the crown–root ratio (Figure 2a). The 3D modified image could also be used to simulate the clinical point of view of the dental practitioner. For non-surgical strategies, the location of the instrument and the long perforation were difficult to perceive on the simulated clinical view. The clinical view of surgical strategies also enables planning possible access ways that avoid sinus perforation (Figure 2b).

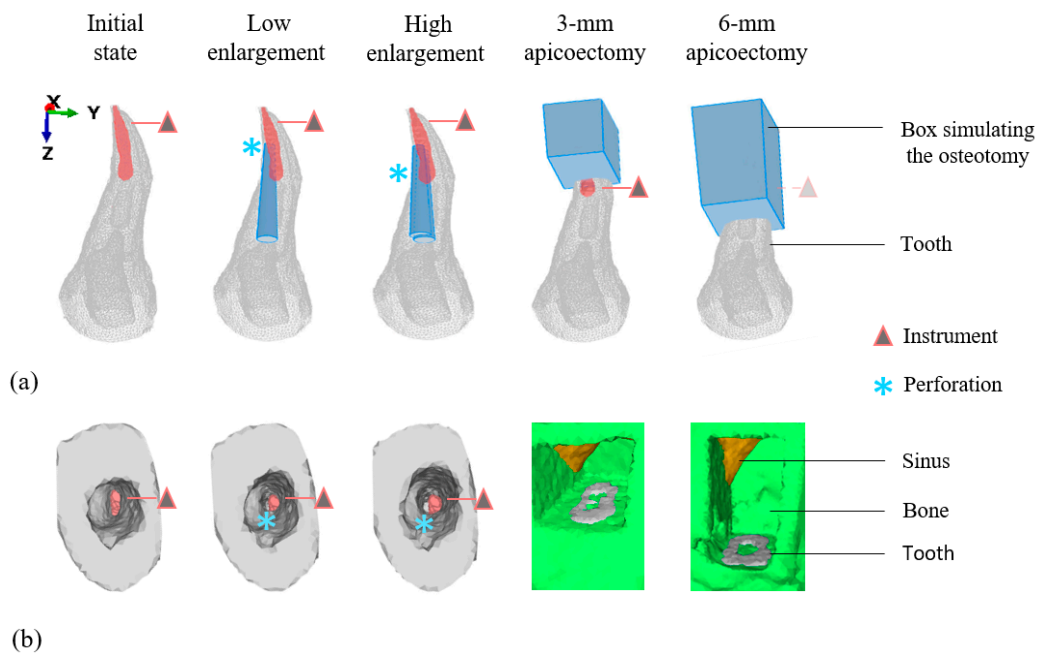


Figure 2. Tri-dimensional images for each situation of the virtual treatment planning. (a) Superimposition on the initial 3D image of the surfaces of the ultrasonic tip for enlargement strategies and osteotomy for apicoectomy strategies. (b) Simulated clinical views of the initial 3D image and of the modified 3D images for each removal strategy.

2.3. Finite Element Modeling and Mechanical Analysis

Modified 3D images were then meshed with tetrahedral elements using the Computational Geometry Algorithms Library (CGAL) meshing library [20] imported in the FEA software Abaqus (Dassault Systèmes, Vélizy-Villacoublay, France; Figure 3). The periodontal ligament could not be detected on the DICOM and was simulated around the root surface with a thickness of 250 μm [21]. The attributed material properties (Table 1) were referenced from the literature [21–23]. All materials were supposed homogeneous, linear and elastic, and there was a perfect bonding between each component [16]. The occlusal faces were not modeled due to X-ray artifacts. A vertical load of 150 N was distributed on the top surface of the root and the nodes of the base, and lateral faces of the bone were constrained to prevent displacement [16]. A static explicit analysis was conducted to calculate principal strains and Von Mises stresses for all FE models. The mechanical behavior of the tooth was evaluated by comparing the Von Mises stress distribution and the maximal Von Mises stress (fracture criterion) [24] between all FE models. Each FE model was verified using a convergence test [25] and the Zhu–Zienkiewicz error estimator [26] (Table 2).

Table 1. Material properties [21–23].

Material	Young’s Modulus (GPa)	Poisson’s Ratio
Dentine	18.6	0.31
Ligament	0.069	0.45
Trabecular bone	1.3	0.3
Gutta	0.069	0.45
Root-end filling (modified zinc-oxide eugenol)	0.1	0.31
Nickel Titanium (ProTaper Gold)	50	0.26

Table 2. Number of elements, nodes, and error indicator according to the finite element model considered.

Structure	Number of Elements	Number of Nodes	Error Indicator Zhu Zienkiewicz
Initial model	202,636	29,742	9.1%
Low enlargement	202,462	29,637	9.2%
High enlargement	202,027	29,614	9.3%
3-mm apicoectomy	201,714	29,855	8.9%
6-mm apicoectomy	207,250	31,126	9.2%

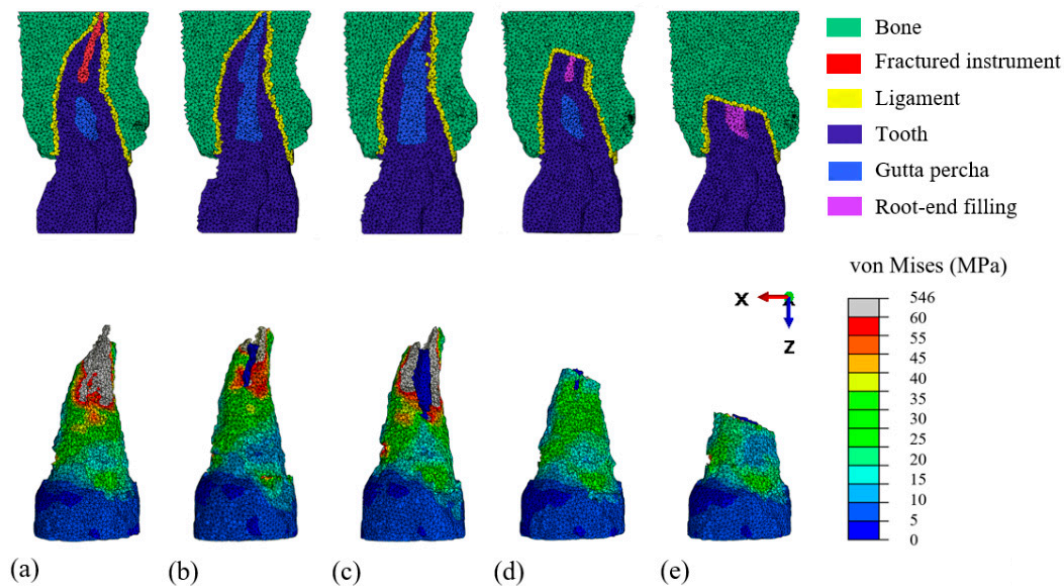


Figure 3. Cut views for each mesh and buccal views of Von Mises root stress represented by color, from blue (low values) to red (high values), for each finite element model. (a) Initial model representing the initial state, (b) low enlargement model, (c) high enlargement model, (d) 3 mm apicoectomy model, and (e) 6 mm apicoectomy model.

The apicoectomy models presented a lower fracture criterion than enlargement models and the model of the initial state of the patient. The 3 mm apicoectomy model presented the lowest value, whereas the high enlargement model presented the highest fracture criterion of all models (Table 3). Regarding stress distribution, high stresses around the instrument were found in the initial model, high stresses around the perforation were found in the enlargement models, and high stresses on the resected surface were found in apicoectomy models (Figure 3). The error indicator was considered as acceptable [27,28] for all models, indicating that this method provides valuable models for FEA.

Table 3. Patient-specific analysis based on the 3D image and maximal Von Mises stress of the different removal strategies.

Clinical Situation	Change on the 3D Initial Image	High Stress Location
Initial state	No	Around the instrument
Low enlargement	Apical perforation	Around the perforation
High enlargement	Lateral perforation	Around the perforation
3 mm apicoectomy	Decrease of the crown root ratio	Resected apex
6 mm apicoectomy	Decrease of the crown root ratio	Resected apex

2.4. Management of the Fractured Instrument

After having informed the patient about the possible treatments, a 3 mm apicoectomy strategy was decided in accordance with her. The orthograde endodontic treatment was completed during the first appointment. The temporary restoration was removed under

isolation with a medium-weight green rubber dam (Hygenic Dental Dam, Coltene, Langenau, Germany). The canal was rinsed with 2.5% sodium hypochlorite, dried, and filled with warm gutta percha and zinc eugenol root canal sealer (EWT, Kerr, Detroit, MI, USA). The tooth was restored using a composite resin (A3 Tetric Evoceram, Ivoclar Vivadent, Saint-Jorioz, France). One week later, the micro apical surgery was conducted following a 3 mm apicoectomy. The root end and the instrument were removed as a single entity to avoid the risk of instrument projection into the sinus [29]. The root end was inspected under high magnification and, in line with the mechanical analysis, no crack or fracture was found. The root canal was treated in a minimally invasive way using only a 3 mm ultrasonic retro-tip (AS3D, Satelec). Then, it was dried with sterile paper points and filled using a polymer-reinforced zinc oxide-eugenol cement (IRM, Dentsply Sirona, Charlotte, NC, USA). The adaptation of the root-end filling was verified on a periapical radiograph, and the flap was closed with 5-0 resorbable sutures (Ethicon Vicryl, Johnson & Johnson, Somerville, NJ, USA). The patient returned to her referent practitioner for prosthetic rehabilitation. The tooth remained asymptomatic at six weeks follow-up and was restored by an inlay. The periapical radiograph at six months and one year showed bone healing and absence of periapical radiolucency (Figure 4).

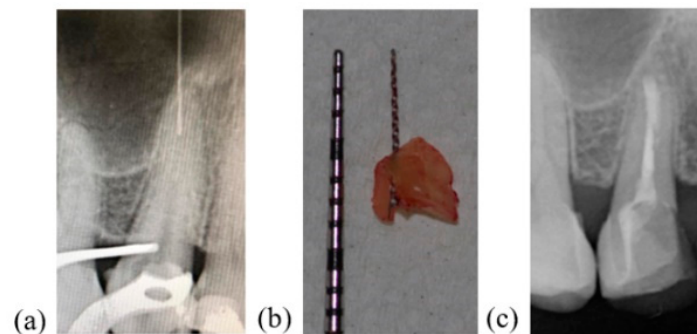


Figure 4. Micro apical surgery of the maxillary premolar. (a) Initial radiograph after instrument fracture, (b) size of the resected apex and of the removed instrument and (c) postoperative radiograph at one year.

3. Discussion

This is the first work to report the use of digital technologies as decision support between non-surgical and surgical strategies of removal of a fractured endodontic instrument. In the present case, the digital approach allowed us to visualize and anticipate the patient-specific root and sinus perforation, and to predict the mechanical impact of four removal strategies.

Studies reported that clinicians have difficulties orienting themselves in space from CBCT slices during their surgical procedure [30]. Herein, VTP was used to simulate the procedures using a multi-label 3D image and to predict the iatrogenicity of the procedure. An increased risk of perforation and complications were reported for the removal of apically fractured instruments [31]. The 3D image enabled us to precisely evaluate the presence of perforation and the position of the sinus using the clinical view. It should be noted that only two endodontic ultrasonic tips were simulated in the current study, but the current proof of concept opens a new way to plan endodontic treatment and develop supplementary digital models of endodontic files. Furthermore, dynamic navigation systems are increasingly being used in the endodontic field [32,33]; a potential application of the current work could therefore be to implement in these systems the developed digital tools and evaluate dynamically their actions on the tooth structure as it is proposed in the medical field [34]. It is of note that the use of a printed guide increases the accuracy and reduces the risk of sinus perforation during endodontic microsurgery [35]. However, this was not used in the case presented herein owing to the risk of instrument projection into the sinus.

In the current case, surgical strategies present a more favorable stress distribution than non-surgical ones, which supports herein the apicoectomy. This conclusion was also recommended by a previous narrative review promoting a surgical approach in cases of a separated instrument in the apical part of the root [3]. However, a first non-surgical attempt to remove the instrument was also advised before considering surgery [5], which makes the decision-making highly complex. Facing this lack of consensus, the benefit of this patient-specific FEA is to optimize an individual's therapy and reduce the risk of root fracture. As a perspective, this patient-specific stress analysis could also lead the root-end preparation to be customized and the tip size to be adapted according to the anatomy of each root [36]. Regarding the resection level, a 3 mm apicoectomy presents lower stresses than 6 mm, which is in accordance with previous FEA studies [9,37]. However, Von Mises stress was herein used as a failure criterion under the assumption that dentin could fail after plastic deformation and distortion [38]. Other criteria such as the maximum of principal stress could have been used to predict fracture and provide different perspectives [38].

Despite the apparent value of the presented strategy, several limitations are to be highlighted. The main one is that the accuracy of CBCT is questionable in the occlusal part due to artifacts, whereas it is known that occlusal morphology influences the stress distribution in FEA [38,39]. Recent technologies such as micro CBCT [40] and the use of an intraoral scanner avoiding X-ray artifacts [41] could improve future simulations. In the present study, the mesh error was considered acceptable [27,28]. However, FEA results should also be carefully interpreted due to the technical impossibility to identify patient-specific parameters such as force intensity [42] or for ligament modeling [43]. Consequently, the use of software in patient care is a debated topic due to the numerous variables involved in the procedure, making standardization highly difficult [25,44]. Artificial intelligence was recently proposed to automatize the segmentation process [45], but the other steps involved in VTP and FEA also require supplementary software and operator skills, which makes their use in routine clinical practice complex. Indeed, the approximate time required could be considered relatively long, but is in good agreement with the mean time required for maxillofacial VTP [46]. From the perspective of endodontic practice, it should be stated that in the maxillofacial field conception time was reduced by 31% compared to a traditional approach [46]. The development of an intuitive software dedicated to the field of endodontics will be necessary in the future to allow a wide dissemination of this technique among dental practitioners.

4. Conclusions

The case presented in this report illustrates some benefits of computer-aided solutions for decision-making in the removal of fractured endodontic instruments by planning the treatment and predicting the mechanical impact induced by non-surgical and surgical strategies. A simulated clinical view and a mechanical failure criterion were successfully used for instrument removal, opening a new way for decision-making in endodontics. Further investigations are, however, required to improve and validate the current methodology for routine clinical practice and to consider supplementary patient-specific parameters.

Author Contributions: All authors made substantial contributions to the present study. R.R. conducted the apical surgery and the finite element analysis. S.V. contributed to image processing. P.B. and M.D. designed the study. R.R., C.V., J.-C.F., and M.D. wrote and edited the manuscript. All authors have read and agreed to the published version of the manuscript.

Funding: This research received no external funding.

Institutional Review Board Statement: The study was conducted according to the guidelines of the Declaration of Helsinki. Since the article is a clinical case report, the ethics committee of the Hospices Civils de Lyon (Lyon University Hospital) ruled that no formal approval by the Ethics Committee was required.

Informed Consent Statement: Written informed consent has been obtained from the patient to publish this paper.

Data Availability Statement: The data presented in this study are available on request from the corresponding author within the framework of a scientific cooperation.

Acknowledgments: The authors would like to thank Philip Robinson (Hospices Civils de Lyon, France) for his help in manuscript preparation.

Conflicts of Interest: The authors declare no conflict of interest.

References

1. Madarati, A.A.; Hunter, M.J.; Dummer, P.M.H. Management of intracanal separated instruments. *J. Endod.* **2013**, *39*, 569–581. [[CrossRef](#)] [[PubMed](#)]
2. Iqbal, M.K.; Kohli, M.R.; Kim, J.S. A retrospective clinical study of incidence of root canal instrument separation in an endodontics graduate program: A PennEndo database study. *J. Endod.* **2006**, *32*, 1048–1052. [[CrossRef](#)]
3. Tzanetakakis, G.N.; Kontakiotis, E.G.; Maurikou, D.V.; Marzelou, M.P. Prevalence and management of instrument fracture in the postgraduate endodontic program at the Dental School of Athens: A five-year retrospective clinical study. *J. Endod.* **2008**, *34*, 675–678. [[CrossRef](#)] [[PubMed](#)]
4. McGuigan, M.B.; Louca, C.; Duncan, H.F. Clinical decision-making after endodontic instrument fracture. *Br. Dent. J.* **2013**, *214*, 395–400. [[CrossRef](#)]
5. Panitvisai, P.; Parunnit, P.; Sathorn, C.; Messer, H.H. Impact of a retained instrument on treatment outcome: A systematic review and meta-analysis. *J. Endod.* **2010**, *36*, 775–780. [[CrossRef](#)]
6. Suter, B.; Lussi, A.; Sequeira, P. Probability of removing fractured instruments from root canals. *Int. Endod. J.* **2005**, *38*, 112–123. [[CrossRef](#)]
7. Setzer, F.C.; Shah, S.B.; Kohli, M.R.; Karabucak, B.; Kim, S. Outcome of endodontic surgery: A meta-analysis of the literature—part 1: Comparison of traditional root-end surgery and endodontic microsurgery. *J. Endod.* **2010**, *36*, 1757–1765. [[CrossRef](#)]
8. Von Arx, T.; Jensen, S.; Bornstein, M. Changes of root length and root-to-crown ratio after apical surgery: An analysis by using cone-beam computed tomography. *J. Endod.* **2015**, *41*, 1424–1429. [[CrossRef](#)] [[PubMed](#)]
9. Jang, Y.; Hong, H.T.; Roh, B.D.; Chun, H.J. Influence of apical root resection on the biomechanical response of a single-rooted tooth: A 3-dimensional finite element analysis. *J. Endod.* **2014**, *40*, 1489–1493. [[CrossRef](#)] [[PubMed](#)]
10. Schestatsky, R.; Dartora, G.; Felberg, R.; Spazzin, A.O.; Sarkis-Onofre, R.; Bacchi, A.; Pereira, G.K.R. Do endodontic retreatment techniques influence the fracture strength of endodontically treated teeth? A systematic review and meta-analysis. *J. Mech. Behav. Biomed. Mater.* **2019**, *90*, 306–312. [[CrossRef](#)]
11. Soares, C.J.; Rodrigues, M.P.; Faria-E-Silva, A.L.; Santos-Filho, P.C.F.; Veríssimo, C.; Kim, H.C.; Versluis, A. How biomechanics can affect the endodontic treated teeth and their restorative procedures? *Braz. Oral Res.* **2018**, *32*, 169–183. [[CrossRef](#)] [[PubMed](#)]
12. Rodby, K.A.; Turin, S.; Jacobs, R.J.; Cruz, J.F.; Hassid, V.J.; Kolokythas, A.; Antony, A.K. Advances in oncologic head and neck reconstruction: Systematic review and future considerations of virtual surgical planning and computer aided design/computer aided modeling. *J. Plast. Reconstr. Aesthetic Surg.* **2014**, *67*, 1171–1185. [[CrossRef](#)]
13. Tang, N.S.J.; Ahmadi, I.; Ramakrishnan, A. Virtual surgical planning in fibula free flap head and neck reconstruction: A systematic review and meta-analysis. *J. Plast. Reconstr. Aesthetic Surg.* **2019**, *72*, 1465–1477. [[CrossRef](#)]
14. Eggermont, F.; van der Wal, G.; Westhoff, P.; Laar, A.; de Jong, M.; Rozema, T.; Kroon, H.M.; Ayu, O.; Derikx, L.; Dijkstra, S.; et al. Patient-specific finite element computer models improve fracture risk assessments in cancer patients with femoral bone metastases compared to clinical guidelines. *Bone* **2020**, *130*, 115101. [[CrossRef](#)]
15. Ni, N.; Ye, J.; Wang, L.; Shen, S.; Han, L.; Wang, Y. Stress distribution in a mandibular premolar after separated nickel-titanium instrument removal and root canal preparation: A three-dimensional finite element analysis. *J. Int. Med. Res.* **2019**, *47*, 1555–1564. [[CrossRef](#)]
16. Kim, S.; Park, S.Y.; Lee, Y.; Lee, C.J.; Karabucak, B.; Kim, H.C.; Kim, E. Stress analyses of retrograde cavity preparation designs for surgical endodontics in the mesial root of the mandibular molar: A finite element analysis; Part I. *J. Endod.* **2019**, *45*, 442–446. [[CrossRef](#)]
17. Gümürükçü, Z.; Kurt, S.; Köse, S. Effect of root resection length and graft type used after apical resection: A finite element study. *J. Oral Maxillofac. Surg.* **2019**, *77*, 1770.e1–1770.e8. [[CrossRef](#)] [[PubMed](#)]
18. Nevares, G.; Cunha, R.S.; Zuolo, M.; da Silveira Bueno, C.E. Success rates for removing or bypassing fractured instruments: A prospective clinical study. *J. Endod.* **2012**, *38*, 442–444. [[CrossRef](#)] [[PubMed](#)]
19. Beldie, L.; Walker, B.; Lu, Y.; Richmond, S.; Middleton, J. Finite element modelling of maxillofacial surgery and facial expressions—A preliminary study. *Int. J. Med. Robot. Comput. Assist. Surg.* **2010**, *6*, 422–430. [[CrossRef](#)]
20. Jacinto, H.; Kéchichian, R.; Desvignes, M.; Prost, R.; Valette, S. A web interface for 3D visualization and interactive segmentation of medical images. In Proceedings of the 17th International Conference on 3D Web Technology, Los Angeles, CA, USA, 4–5 August 2012; Volume 17, pp. 51–58.
21. Chang, Y.H.; Lee, H.; Lin, C.L. Early resin luting material damage around a circular fiber post in a root canal treated premolar by using micro-computerized tomographic and finite element sub-modeling analyses. *J. Mech. Behav. Biomed. Mater.* **2015**, *51*, 184–193. [[CrossRef](#)]
22. Thompson, S.A. An overview of nickel—Titanium alloys used in dentistry. *Int. Endod. J.* **2000**, *33*, 297–310. [[CrossRef](#)]

23. Hondrum, S.O. Temporary dental restorative materials for military field use. *Mil. Med.* **1998**, *163*, 381–385. [[CrossRef](#)] [[PubMed](#)]
24. Juloski, J.; Apicella, D.; Ferrari, M. The effect of ferrule height on stress distribution within a tooth restored with fibre posts and ceramic crown: A finite element analysis. *Dent. Mater.* **2014**, *30*, 1304–1315. [[CrossRef](#)] [[PubMed](#)]
25. Erdemir, A.; Guess, T.M.; Halloran, J.; Tadepalli, S.C.; Morrison, T.M. Considerations for reporting finite element analysis studies in biomechanics. *J. Biomech.* **2012**, *45*, 625–633. [[CrossRef](#)]
26. Zhu, J.Z.; Zienkiewicz, O.C. A posteriori error estimation and three-dimensional automatic mesh generation. *Finite Elem. Anal. Des.* **1997**, *25*, 167–184. [[CrossRef](#)]
27. Fischer, A.; Eidel, B. Convergence and Error Analysis of FE-HMM/FE for energetically consistent micro-coupling conditions in linear elastic solids. *Eur. J. Mech. A/Solids* **2019**, *77*, 103735. [[CrossRef](#)]
28. Fischer, A.; Eidel, B. Error analysis for quadtree-type mesh coarsening algorithms adapted to pixelized heterogeneous microstructures. *Comput. Mech.* **2020**, *65*, 1467–1491. [[CrossRef](#)]
29. Hauman, C.H.J.; Chandler, N.P.; Tong, D.C. Endodontic implications of the maxillary sinus: A review. *Int. Endod. J.* **2002**, *35*, 127–141. [[CrossRef](#)]
30. Scarfe, W.C.; Levin, M.D.; Gane, D.; Farman, A.G. Use of cone beam computed tomography in endodontics. *Int. J. Dent.* **2009**, *2009*, 634567. [[CrossRef](#)]
31. Parashos, P.; Messer, H.H. Rotary NiTi instrument fracture and its consequences. *J. Endod.* **2006**, *32*, 1031–1043. [[CrossRef](#)]
32. Gambarini, G.; Galli, M.; Stefanelli, L.; Di Nardo, D.; Morese, A.; Seracchiani, M.; De Angelis, F.; Di Carlo, F.; Testarelli, L. Endodontic microsurgery using dynamic navigation system: A case report. *J. Endod.* **2019**, *45*, 1397–1402. [[CrossRef](#)] [[PubMed](#)]
33. Zubizarreta-macho, Á.; De Pedro, M.A.; Deglow, E.; Agustín-Panadero, R.; Mena Álvarez, J. Accuracy of computer-aided dynamic navigation compared to computer-aided static procedure for endodontic access cavities: An in vitro study 2020. *J. Clin. Med.* **2020**, *1*, 2–9.
34. Herford, A.S.; Miller, M.; Lauritano, F.; Cervino, G.; Signorino, F.; Maiorana, C. The use of virtual surgical planning and navigation in the treatment of orbital trauma. *Chin. J. Traumatol.* **2017**, *20*, 9–13. [[CrossRef](#)] [[PubMed](#)]
35. Giacomino, C.M.; Ray, J.J.; Wealleans, J.A. Targeted Endodontic Microsurgery: A Novel Approach to Anatomically Challenging Scenarios Using 3-dimensional—Printed Guides and Trepine Burs—A Report of 3 Cases. *J. Endod.* **2018**, *44*, 1–7. [[CrossRef](#)] [[PubMed](#)]
36. Palma, P.J.; Marques, J.A.; Casau, M.; Santos, A.; Caramelo, F.; Falacho, R.I.; Santos, J.M. Evaluation of Root-End Preparation with Two Different Endodontic Microsurgery Ultrasonic Tips. *Biomedicines* **2020**, *8*, 383. [[CrossRef](#)]
37. Ran, S.J.; Yang, X.; Sun, Z.; Zhang, Y.; Chen, J.X.; Wang, D.M.; Liu, B. Effect of length of apical root resection on the biomechanical response of a maxillary central incisor in various occlusal relationships. *Int. Endod. J.* **2020**, *53*, 111–121. [[CrossRef](#)]
38. Richert, R.; Farges, J.C.; Tamimi, F.; Naouar, N.; Boisse, P.; Ducret, M. Validated finite element models of premolars: A scoping review. *Materials* **2020**, *13*, 3280. [[CrossRef](#)]
39. Benazzi, S.; Grosse, I.R.; Gruppioni, G.; Weber, G.W.; Kullmer, O. Comparison of occlusal loading conditions in a lower second premolar using three-dimensional finite element analysis. *Clin. Oral Investig.* **2014**, *18*, 369–375. [[CrossRef](#)]
40. Murakami, N.; Wakabayash, N. Finite element contact analysis as a critical technique in dental biomechanics: A review. *J. Prosthodont. Res.* **2014**, *58*, 92–101. [[CrossRef](#)]
41. Acar, B.; Kamburoğlu, K.; Tatar, I.; Arıkan, V.; Çelik, H.H.; Yüksel, S.; Özen, T. Comparison of micro-computerized tomography and cone-beam computerized tomography in the detection of accessory canals in primary molars. *Imaging Sci. Dent.* **2015**, *45*, 205–211. [[CrossRef](#)] [[PubMed](#)]
42. Rangel, F.A.; Maal, T.J.J.; Bronkhorst, E.M.; Breuning, K.H.; Schols, J.G.J.H.; Bergé, S.J.; Kuijpers-Jagtman, A. M Accuracy and reliability of a novel method for fusion of digital dental casts and cone beam computed tomography scans. *PLoS ONE* **2013**, *8*, e59130. [[CrossRef](#)] [[PubMed](#)]
43. Papadopoulou, K.; Hasan, I.; Keilig, L.; Reimann, S.; Eliades, T.; Jäger, A.; Deschner, J.; Bourauel, C. Biomechanical time dependency of the periodontal ligament: A combined experimental and numerical approach. *Eur. J. Orthod.* **2013**, *35*, 811–818. [[CrossRef](#)] [[PubMed](#)]
44. Cervino, G.; Fiorillo, L.; Arzukanyan, A.V.; Spagnuolo, G.; Campagna, P.; Cicciù, M. Application of bioengineering devices for stress evaluation in dentistry: The last 10 years FEM parametric analysis of outcomes and current trends. *Minerva Stomatol.* **2020**, *69*, 55–62. [[CrossRef](#)] [[PubMed](#)]
45. Lahoud, P.; EzEldeen, M.; Beznik, T.; Willems, H.; Leite, A.; Van Gerven, A.; Jacobs, R. Artificial intelligence for fast and accurate 3D tooth segmentation on CBCT. *J. Endod.* **2021**. [[CrossRef](#)] [[PubMed](#)]
46. Wrzosek, M.K.; Peacock, Z.S.; Laviv, A.; Goldwasser, B.R.; Ortiz, R.; Resnick, C.M.; Troulis, M.J.; Kaban, L.B. Comparison of time required for traditional versus virtual orthognathic surgery treatment planning. *Int. J. Oral Maxillofac. Surg.* **2016**, *45*, 1065–1069. [[CrossRef](#)] [[PubMed](#)]